Mechanical Systems and Signal Processing 109 (2018) 45–57

Contents lists available at ScienceDirect

Mechanical Systems and Signal Processing

journal homepage: www.elsevier.com/locate/ymssp

Prognosability study of ball screw degradation using systematic methodology

Pin Li [a], Xiaodong Jia [a,*], Jianshe Feng [a], Hossein Davari [a], Guan Qiao [b], Yihchyun Hwang [c], Jay Lee [a]

[a] NSF I/UCR Center for Intelligent Maintenance Systems, Department of Mechanical Engineering, University of Cincinnati, PO Box 210072, Cincinnati, OH 45221-0072, USA
[b] ShanXi Engineering Laboratory for Transmissions and Controls, Northwestern Polytechnical University, Xi'an, China
[c] HIWIN Technologies Corp., No. 7, Jingke Rd., Taichung Precision Machinery Park, Taichung 40852, Taiwan

ARTICLE INFO

Article history:
Received 1 December 2017
Received in revised form 2 February 2018
Accepted 25 February 2018

Keywords:
Prognosability
Prognosis and health management
Data quality
Ball screw
Sensor-less
Sensor-rich

ABSTRACT

As a critical mechanical component that converts rotary motion to linear motion with high precision, the ball screw has drawn a lot of attention in the field of Prognostics and Health Management (PHM). However, prognosis of the ball screw degradation has not been fully discussed yet in the current literature. This paper first justifies the prognosability of a ball screw via experimental studies, then proposes a systematic methodology for ball screw prognosis to implement the fault diagnosis, early diagnosis, health assessment and remaining useful life (RUL) prediction. Meanwhile, sensor-less and sensor-rich strategies are investigated and benchmarked in the experimental studies. The results demonstrate that the ball screw degradation behavior is available for prognosis and the proposed methodology can effectively help users to implement PHM analysis. Besides, the benchmark studies between sensor-less and sensor-rich strategies also achieve several practical conclusions that are valuable for real-world applications.

1. Introduction

The ball screw is an important mechanical device that is widely employed to convert rotary motion to linear motion with high precision. Application of ball screws can be found in many engineering systems which require very precise position control, such as the feed drive system for a machine tool and the high precision leveling system for aircrafts and missiles. In practice, it is found that the operation risks may increase significantly as the ball screw assembly degrades over time, since the ball screw degradation can have a huge impact on the control precision. For example, the preload loss will reduce the stiffness of the ball screw assembly and eventually such kind of degradation would lead to position accuracy loss. Therefore, prognosis of the ball screw holds great practical and academic value.

Prognosis of the ball screw is intrinsically challenging due to the complex motion trajectory of the rolling elements and the limited space for sensor installation. To monitor the preload loss, one simple way is to install a force sensor to measure the no-load torque of the ball nut. However, this method is rendered impractical due to the cost of the force sensors and the complication of sensor installation. As an alternative solution, Hilbert-Huang Transform (HHT) and Multiscale entropy (MSE) analysis are utilized to process vibration data for diagnosing the different ball screw preload levels [1]; vibration energy at a

* Corresponding author at: 560 Baldwin Hall, University of Cincinnati, PO Box 210072, Cincinnati, OH 45221, USA.
E-mail address: jiaxg@mail.uc.edu (X. Jia).

https://doi.org/10.1016/j.ymssp.2018.02.046
0888-3270/

specific frequency range is also proposed to diagnose different preload loss levels [2]. Considering the vibration signal contamination from other components like bearings, which is not related to ball screw preload, Angular Velocity Vold-Kalman Filtering Order Tracking (AVVKF-OT) was proposed to isolate vibration signals merely from the ball screw nut and then ball pass frequency was used to detect the onset of preload loss [3]. To study the feature extraction strategy from vibration data, Jin et al. [4] proposes to apply a wide range of signal processing techniques to extract features from the time domain, frequency domain and time-frequency domain, then use Fisher Criterion to select the most effective features to diagnose different preload levels. Besides the vibration analysis, built-in signals from controller have been also explored. The Hilbert-Huang Transform (HHT) and Multiscale entropy (MSE) analysis have been employed to process the motor current signal for preload loss diagnosis [5].

Summarizing the related works in current literature, it is found that most of the previous works mainly focus on the diagnosis of ball screw failures and the exploration of the fault mechanism. However, prognosis of the ball screw degradation has not been fully discussed yet in the current literature. According to the '5C' framework for machine prognostics and health management (PHM) that is depicted in Ref. [6], machine prognosis should include fault diagnosis, early diagnosis, health assessment and remaining useful life (RUL) prediction. Before the PHM implementations, feasibility studies are needed to justify the prognosability of the system [7]. To study the ball screw degradation systematically, this research aims to address the following two engineering problems: (1) to justify the availability of ball screw for prognostic analysis; (2) to propose a systematic methodology for ball screw fault diagnosis, early diagnosis, health assessment and RUL prediction. Besides, this research also investigates the necessity of add-on accelerometers for PHM purpose.

To tackle these engineering problems, this research first designs new experiments to study the degradation behavior of a ball screw and then proposes a systematic methodology for ball screw prognosis. The contribution of this paper can be summarized from four aspects: (1) two different experimental studies are designed respectively to discuss the availability of prognostics and to validate the effectiveness of the proposed prognosis methodology. The prognosability of the ball screw system is justified by diagnosing the system degradation at different severity levels in Experiment 1 and the effectiveness of the proposed method is demonstrated by the accelerated life test (ALT) in Experiment 2; (2) a systematic methodology for the ball screw prognosis is proposed and validated. To make the proposed methodology more practical and robust, only the off-the-shelf machine learning algorithms are employed; (3) the sensor-less strategy (using built-in sensors only) and sensor-rich strategy (using extra accelerometers) for PHM analysis are benchmarked in all the case studies. (4) Conclusions made in this work hold great practical value, which clearly indicates the suitable signal sources for ball screw prognosis based on the proposed methodology.

The rest of this paper is organized as follows; The engineering problems to be addressed in this study are clearly stated in Section 2. Section 3 elaborates on the experimental studies as well as the proposed methodology. In Section 4, the analysis results are presented and discussed. The conclusion remarks are presented in Section 5.

2. Problem statement

The ball screw preload condition has major impacts on the system stiffness and will eventually affect the manufacturing precision as the mechanical parts wear out. In practice, preload loss is observed as one of the most common phenomena for ball screw degradation, and the preload condition of the ball nut and guideway will get worse over time. However, the monitoring of preload loss is still challenging since the motion of a ball screw in operation is non-stationary and dynamic. Vibration analysis has been explored in the recent literature to detect the preload loss. GH. Feng et al. [8] proposes a dynamic model of a ball screw preload adjustable feed drive system to build the relationship between preload variation and vibration signal spectrum during the operation. Tsai et al. proposes a ball pass frequency detection method using Angular Velocity Vold–Kalman Filtering Order Tracking (AVVKF-OT), by which the onset of ball screw preload loss is identified [3]. However, it is found that the vibration data from harsh manufacturing environments can be easily contaminated by the unwanted noise [8,9] and also it is challenging to directly sense the ball nut vibration due to the accessibility of the space [10]. To unveil these obscurities, this research compares both the sensor-rich and sensor-less strategies for ball screw PHM analysis. The sensor-less strategy only relies on the built-in speed and torque signal from controller, while the sensor-rich strategy considers data from both the controller and the add-on accelerometers. To make the PHM analysis for the ball screw assembly comprehensive, the preload conditions of both ball screw and guideway are investigated at three different levels – good preload condition, mildly degraded and fully degraded.

This research studies the ball screw PHM following the framework in Fig. 1 and primarily focuses on the early diagnosis, health assessment and RUL prediction of the ball screw assembly. Early diagnosis in this research includes accurate classification of different failure modes (primarily ball-nut preload loss and guideway preload loss) at different degradation levels. The early diagnosis study is introduced first since it builds the foundation for subsequent PHM analysis. As depicted in Fig. 1, the ability to classify the different degradation levels is a pre-requisite of the subsequent health assessment, which justifies the availability of prognosis for the ball screw assembly [11]. To study the early diagnosis of the system and justify the availability for subsequent prognosis tasks, a number of comparative test runs are designed in Experiment 1 which will be detailed in next section. The health assessment and RUL prediction aim to model the slow degradation of the ball-screw assembly using a univariate health series and then predict the RUL of the system based on the health series, as shown in

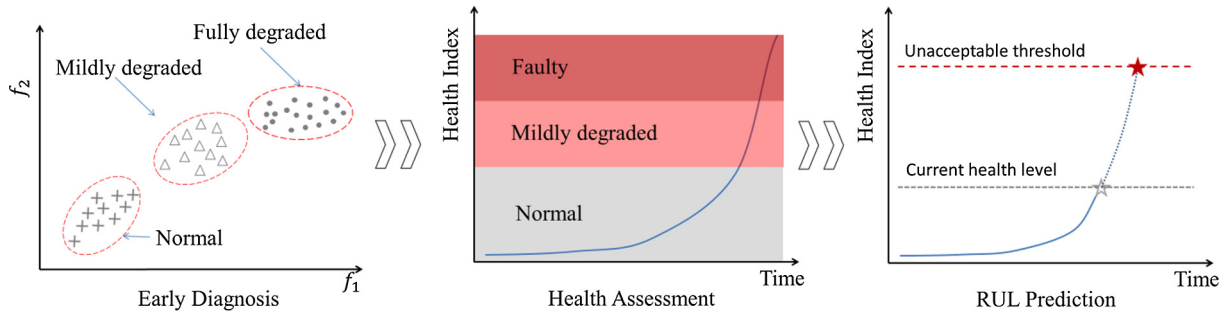

Fig. 1. Framework for the PHM analysis for the ball screw assembly.

Fig. 1. To justify the effectiveness, one accelerated life test (ALT) is designed in Experiment 2, which will be introduced in the next section also.

PHM analysis for ball screw degradation embraces two different methodologies – the physics based approaches and the data driven approaches, according to a number of recent studies [3,12,13]. Previous research on physics based approaches dive deep into the fault mechanism and attempt to derive an equation of ball pass frequency (BPF) to study the preload loss. However, due to the complex motion trajectory of the rolling mechanism, an explicit function for BPF is intrinsically challenging and there is still no generally accepted equation for BPF in the literature [3,14]. Therefore, this research focuses mainly on data driven approaches. We employ the off-the-shelf data driven approaches only to make this research more practical for the engineering community.

3. Experimental studies and methodology

3.1. Design of experiments

As shown in Fig. 2, for this experiment the ball screw module is fixed on a concrete base and is running along the horizontal guideway during the test. The specification of the test bed is listed in Table 1. In this experimental investigation, the built-in speed and torque signal from the controller are collected and the sampling rate for these built-in signals is 25.6 kHz. Besides the controller data, three accelerators are installed on the ball screw nut, front and end of the bearing base to measure the vibration of these key components, as shown in Fig. 2. The vibration data is collected by the NI9234 data acquisition card and the sampling rate is set to 25.6 kHz. The collected vibration data and controller data are saved as TDMS data files for further analysis. In this work, two experiments are designed for different purposes to address the engineering challenges discussed above.

To justify the availability of the ball screw prognosis, the first experiment aims to verify whether the data from different degradation levels can be classified by the off-the-shelf machine learning tools. In this experimental investigation, three guideways and three ball screws with different preload levels are provided by HIWIN as listed in Table 2.

To create a simplified visualization tool, many manufacturing industries prefer to use three different stages (Green Zone, Yellow Zone, Red Zone) to describe the health condition of machine tools or critical components. The Green Zone indicates that machine tools or critical components are in a healthy condition and that no further attention is needed for normal operation. The Yellow Zone indicates that machine tools or critical components are in a mildly degraded condition, and although they can still operate normally, potential failure would happen in the near future due to degradation, thus, further attention is needed. Finally, the Red Zone indicates that machine tools or critical components are in a faulty condition, they need to be replaced or repaired before being used in a production line. To normalize this research to the manufacturing industry trends, 3 levels of different preload conditions for both the ball screw and the guideway were used in this research. Based on

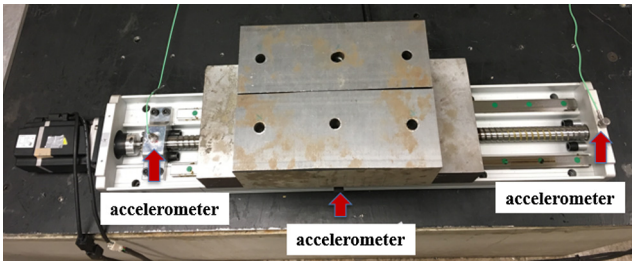

Fig. 2. Ball screw test bed.

Table 1
Test bed specification.

Test bed component	Specification	Dynamic load
Ball screw	R25-10 K3-FSC-724-815-0.018	1260 kgf
Guideway	HGH20CA2R716ZAC	1810 kgf
Motor	FRLS-4020506A	NA
Controller	D2T-0423-E-B0	NA

Table 2
Equipment list for experiment 1.

Ball screw			Guideway		
ID	Degradation level	Preload condition	ID	Degradation level	Preload condition
A	Normal	50.4 kgf	G	Normal	108.6 kgf
B	Mildly degraded	12.6 kgf	Y	Mildly degraded	24.1 kgf
C	Faulty	Backlash 12 μm	R	Faulty	Backlash 18 μm

discussions with the ball screw design expert at HIWIN, the specific kgf numbers for different preload conditions are settled upon the company technical report [15,16]. In this experiment, normal ball screw has the 4% preload level (4% $*$ 1260 kgf = 50.4 kgf) and normal guideway has the 6% preload level (6% $*$ 1810 kgf = 108.6 kgf).

It's noted that all degradations are caused by field usage instead of manually seeded in the ball screw assembly, which guarantees the fidelity of the ball screw degradation analysis. To obtain a comprehensive understanding of the system degradation, 9 comparative experiments are designed, using different combinations of the ball screw and the guideway, as tabulated in Table 3. For each test run, the ball screw assembly is running through the same speed level (400 mm/s) to collect data. The ball screw assembly is kept running constantly under the specified speed level for 1 h. 10 s of data are collected at each minute during the 1 h running test for every ball screw assembly. To ensure that the ball screw assembly is operating under a stable condition during the tests, each ball screw assembly will run 30 min before data collection and sufficient lubrication is provided throughout the experiment.

The second experiment is designed to investigate the degradation process of the ball screw assembly, and one accelerated life test is designed based on a completely new ball screw assembly. In order to accelerate the degradation process, the movement of the ball screw is restricted to the second half of the full stroke (away from the motor). It's worth noting that this half stroke movement simulates the actual ball screw usage inside the CNC machine tools. In addition, a 100 kg load is added to the work table that is located on top of the ball nut. Throughout the ALT, no further lubrication is provided except at the very beginning of the test. During the ALT, the ball screw assembly is kept running at 400 mm/s constantly for 24 h a day and 7 days a week. Controller data and vibration data are collected at each hour, and each data collection lasts 1 min. All the data throughout the experiment is collected with sampling rate of 25.6 kHz. At the end of the ALT, it is found that the ball screw degrades at a faster rate than the guideway. After consultation with ball screw users in industry, this observation correlates with the frequent failure modes seen in the industrial usage of the ball screw inside the CNC machine tools. This correlation helps to validate the effectiveness of the designed ALT experiment for simulating the actual degradation process in a manufacturing scenario.

3.2. The proposed methodology

The overall methodology proposed for this study is depicted in Fig. 3. The data collected during the study include the vibration data from three accelerometers in Fig. 2 and the built-in speed and torque signals from the controller. Due to the structural differences compared to the typical rotating components like a bearing and a gearbox, ball screw's movement

Table 3
List of 9 comparative test runs.

Experiment ID	Balls screw and guideway combination
1	A-G
2	A-Y
3	A-R
4	B-G
5	B-Y
6	B-R
7	C-G
8	C-Y
9	C-R

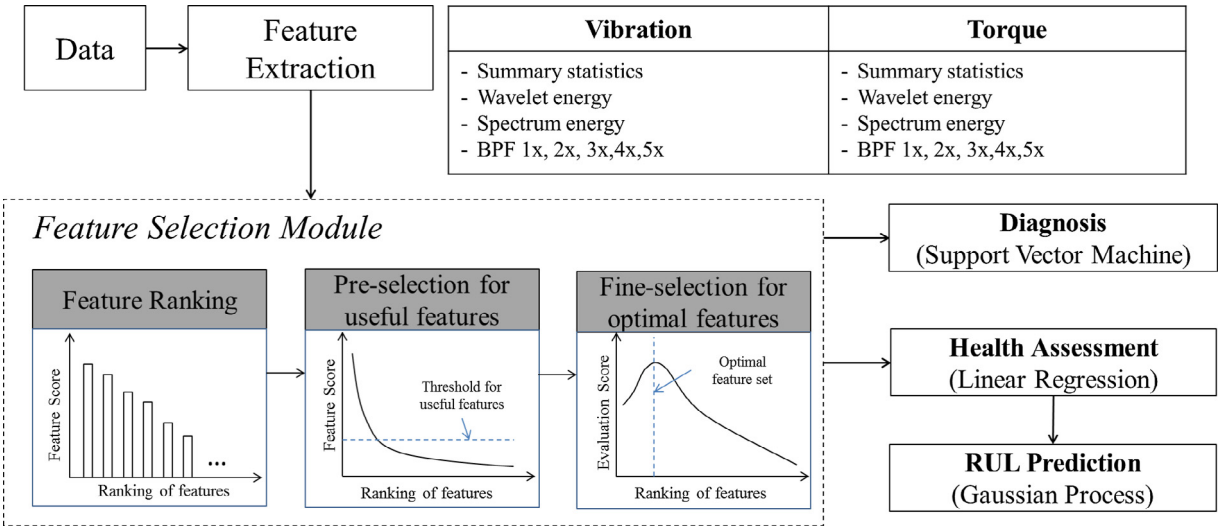

Fig. 3. Data processing pipeline for the smart field agent.

pattern is usually segmented by cycle, which contains a full-stroke forward and a full-stroke backward movement. In the full-stroke forward movement, the ball screw will first accelerate to a specified speed using constant acceleration, then will run on the guideway with a constant speed for a while, and finally will decelerate and stop at the other end of the stroke. The backward movement has the same movement pattern with an opposite direction. In this research, segmentation techniques are employed to the raw data to filter out the constant speed part from both forward and backward movement, from which a wide variety of feature extraction methods are used.

For each data channel, the features are extracted in the time domain, frequency domain and the time frequency domain. For the time domain features, the summary statistics, such as RMS, mean, variance, Kurtosis and Skewness, are mainly computed. For the frequency domains, energy is extracted from different frequency bands: [0, 0.5 kHz], [0.5 kHz, 1 kHz], [1 kHz, 2 kHz], [2 kHz, 6 kHz], [6 kHz, 12.8 kHz]. Amplitudes at the ball screw rotation frequency and its harmonics are also used as features. Also, amplitude at the calculated ball passing frequency (BPF) based on Eqs. (1)–(4) given by [3] and amplitudes at BPF harmonics are used as frequency features.

$$\frac{w_m}{w_b} = \frac{1}{1 + \frac{(1+\gamma\cdot\cos\alpha_o)(\tan\beta\cdot\sin\alpha_i+\cos\alpha_i)}{(1-\gamma\cdot\cos\alpha_i)(\tan\beta\cdot\sin\alpha_o+\cos\alpha_o)}} \tag{1}$$

$$\gamma = \frac{r_b}{r_m} \tag{2}$$

$$2r_b = r_m\sqrt{2(1-\cos\varphi) + (\varphi\cdot\tan\alpha)^2} \tag{3}$$

$$BPF = \frac{w_m}{\varphi} \tag{4}$$

where w_m is the moving ball rotational speed, w_b is the ball screw rotational speed, γ is the ratio of ball radius r_b to the pitch circle radius r_m, and α_o is the ball screw contact angle with nut, α_i is the ball screw contact angle with screw and $\alpha_o \approx \alpha_i$. β can be assumed to be 47.5^o and α is the helix angle of ball screw raceway, thus BPF can be determined for a specific ball screw.

For the time frequency domain, based on the previous experience on applying wavelet decomposition to the time varying signal, wavelet decomposition at level 4 using 'db4' wavelet is performed on each data channel and the energy at each level is used as a feature [17]. At the end of the feature extraction step, 440 features in total are extracted from the raw data. Since the feature extraction part is quite standard compared to our previous publications [18–20], this research adds more emphasize on the feature selection strategies. Based on current literature, common feature selection methods can be categorized into two families: the filter-based and the wrapper based approaches. The filter based approach ranks the features first using pre-selected ranking criterion and then selects important features by its ranking scores. The wrapper method selects the feature subset based on the given classifier or regression method and various searching method such as forward search, backward search are proposed [21]. To find a practical feature selection strategy for PHM application, this study explores a hybrid strategy for feature selection. In Fig. 3, the incoming features are first ranked using pre-selected ranking criterion. Next, the useful feature set is selected. This is done by keeping the features that have scores higher than the empirical threshold. It is

important to mention that the useful feature set should be comprehensive and therefore a relatively smaller threshold is suggested in this step. After the pre-selection of the useful features, a finer selection is suggested by using wrapper approaches based on the given classifier or regression method. The searching space for the wrapper approach is the selected useful features and the search sequence is based on the ranking score from high to low. In the fine-selection step in Fig. 3, an evaluation criterion is needed to decide how many features can be selected as an optimal feature set for the subsequent modeling steps. After the feature selection, diagnosis and prediction models can be constructed using data-driven approaches. In this study, only the off-the-shelf machine learning algorithms are employed to build health models for the ball screw.

Since the class information for training data is always available, feature selection for classification, or fault diagnosis and early diagnosis, is straightforward and the fisher score shown below is widely employed for feature ranking [22].

$$S_c = \frac{\sum_{k=1}^{c} n_k (\mu_k^j - \mu^j)^2}{\sum_{k=1}^{c} n_k (\sigma_k^j)^2} \tag{5}$$

where c means the number of classes, n_k means the number of samples in k-th class. μ_k^j and σ_k^j are the mean and standard deviation of the k -th class, corresponding to the j -th feature, μ^j denotes the mean of the whole data set corresponding to the j-th feature. $(\mu_k^j - \mu^j)^2$ represents the distance between each class and the center of the whole data set, higher value would lead to easier differentiation of the multiple classes. $(\sigma_k^j)^2$ represents the disperse degree of each class data, usually smaller value would lead to a good classification result. However, in practice, it is found that the feature ranking using fisher scores for multi-class classification problem might be biased in some scenarios and is only appropriate for the pre-selection of useful features. This is also the reason why finer selection is introduced subsequently. The fisher ranking, however, is still quite useful in this study to boost the efficiency of wrapper searching by defining a smaller space for searching and also a sequence for searching. In the fine-selection step, the overall classification accuracy of the SVM is employed to select the optimal feature set for diagnosis.

Feature selection for prognosis is not as straightforward as the diagnosis problem and there are several things that need to be considered. Firstly, the relationship among useful feature spaces for prognosis, early diagnosis and diagnosis is described in Fig. 4 and the useful features for prognosis must be also useful for early diagnosis and fault diagnosis. Therefore, in the pre-selection of the useful features for prognosis, the useful features for early diagnosis need to be identified and re-ranked. Second, the ranking criterion needs to consider the monotonicity of the feature, the features with good monotonicity are found to be important to the health assessment and RUL prediction since the machine degradation is normally recognized as a slow and monotonic process that may span months or year [23]. Therefore, the slope value described below is employed to rank all the features for preselection:

$$S_p = \frac{\sum_k (x_k - \bar{x})(y_k - \bar{y})}{\sum_k (x_k - \bar{x})^2}, \quad \text{where } \bar{x} = \frac{1}{n}\sum_k x_k, \bar{y} = \frac{1}{n}\sum_k y_k, \quad k = 1, \ldots, n \tag{6}$$

where n means number of observations, and the S_p represents the slope of the linear regression for individual feature. In the setting of this study, the x_k means the k -th time point and y_k represents the feature value at time k. Although the use of S_p for feature monotonicity ranking is intuitive, this measure is found to be an effective regularizer for the Restricted Boltzmann Machine (RBM) to enhance RUL prediction accuracy [23]. The slope value employed in this investigation is mainly due to its robustness to the noise in the feature series and a larger value of the slope value intuitively means better monotonicity of the feature. To make the slope value comparable for features with different scale, all the features are normalized to zero-mean and unitary variance prior to the feature pre-selection.

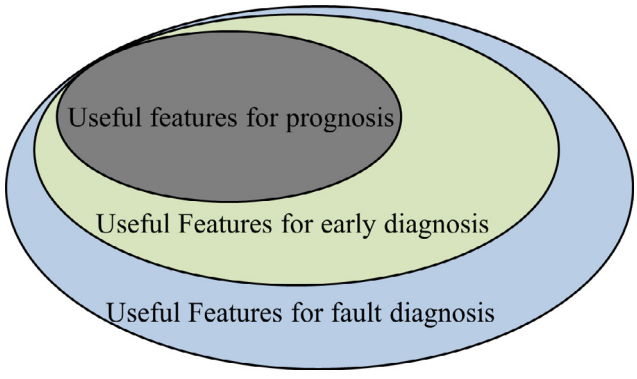

Fig. 4. Relationship among the useful feature sets for prognosis, early diagnosis and fault diagnosis.

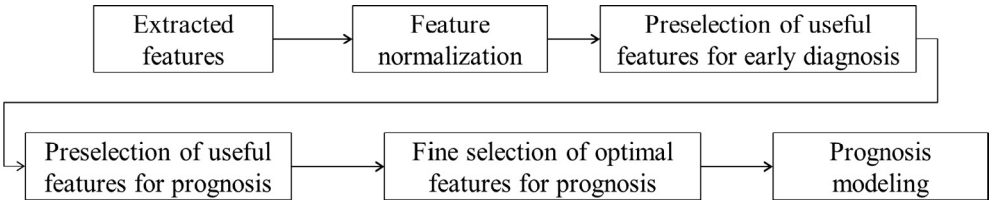

Fig. 5. Pipeline of analysis for prognosable feature selection strategy.

To select an optimal feature set for health assessment modeling, the evaluation measure evaluates both the trend-ability and the noisiness of the estimated degradation trajectory for fine selection. The degradation trajectory is estimated by the trained degradation model based on linear regression and the model is trained by setting the health level of the first 24 h to be 0.95 and the last 24 h to be 0.05. The estimated degradation trajectory is often very noisy with a slow downward trend superimposed with random noise. To evaluate the performance of the degradation assessment, the Mann-Kendall (MK) test [24] is employed to evaluate the monotonicity of the trend component and the signal-to-noise ratio (SNR) is utilized to assess the noisiness of the degradation trajectory. In this study, the trend component of the degradation trajectory is extracted using Gaussian Process Regression (GPR) and the noise term is regarded as the remaining component of the trajectory, which can be described below:

$$H_{tr} = E[H_*|H, t, t_*] \tag{7}$$

$$H_{no} = H - H_{tr} \tag{8}$$

$$\mathrm{SNR} = 10 * \log_{10} \frac{P_{tr}}{P_{no}} \tag{9}$$

where Eq. (7) is a simple mathematical description of using GPR model for prediction. The variable t and H in Eq. (7) denote the time stamp and the noisy degradation trajectory given by the degradation assessment model. The t_* and H_* in Eq. (7) denotes the time stamp and health value that is to be predicted by the GPR model. To extract the trend term H_{tr} of H, the t_* in Eq. (7) is set the same as t. After the trend component H_{tr} is estimated, the noise component H_{no} can subsequently be estimated and the SNR can also be calculated using Eq. (9), where P_{tr} and P_{no} denotes the signal power of the trend term H_{tr} and the noise term H_{no} respectively. By searching through all the useful features in the preselection step, the optimal feature set for degradation assessment can be determined by finding the maximum SNR value under the condition that the degradation trend H_{tr} is tested as monotonic by MK test.

As a summary, the general steps for prognosable feature selection is sketched in Fig. 5. To select an optimal feature set for prognosis, the usefulness of the selected features for early diagnosis needs to be considered first and the its usefulness for prognosis is ranked preliminarily using the slope value in Eq. (6). After the preselection steps, the fine selection decides the optimal feature set using evaluation criterion in Eqs. (7)–(9).

4. Results and discussions

4.1. Case study 1: early diagnosis of ball screw degradation

Fig. 6 presents the feature ranking based on the fisher score. In the setting of binary classification, fisher score larger than 1 means the feature is valuable for the classifier. However, for multi-class classification problem, selection of a proper threshold is not that straightforward. In this study, this threshold is empirically set to 9 since there are 9 classes in total in the dataset. All the features whose scores higher than 9 are selected as useful features.

The results of the fine selection for the optimal feature set are presented in Fig. 7. In Fig. 7, the y-axis plots the classification accuracy given the 10-fold cross validation (CV) based on the support vector machine (SVM). The three curves are obtained by the forward search strategy, which follows the ranking given by the fisher score. One can easily see where there is an optimal point in the curves that decides the optimal feature set for classification and all the optimal accuracy is close to 100%. This demonstrates that the ball screw assembly is available for early diagnosis and thus subsequent prognosis.

Another observation in Fig. 7 is that the CV accuracy using the controller features is better than the vibration features, which clearly indicates that the built-in signals from the controller are sufficient for the ball screw early diagnosis. To further discuss this, the top-ranking features from the torque signal and the vibration signal are compared in Fig. 8. Fig. 8(a) demonstrates the best feature from the torque signal which separates the 9 different classes. Fig. 8(b) shows the best feature from the vibration signal at the ball nut. One can see that this feature can also separate most classes very well but still includes some mixed points. Comparing the fisher score of these two features indicates that the vibrational feature in Fig. 8(b) is assigned for a larger fisher score. This is because the use of the fisher score for feature selection might be biased for

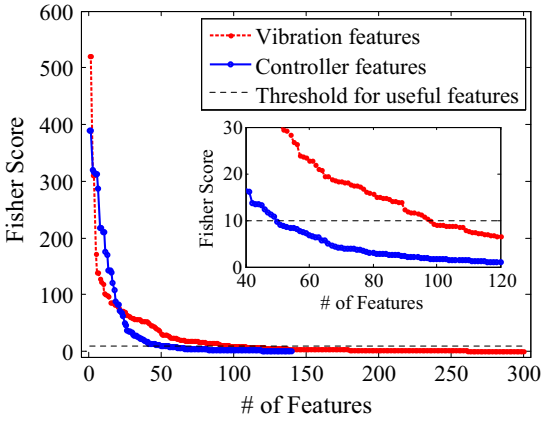

Fig. 6. Preselection for the useful feature set for early diagnosis.

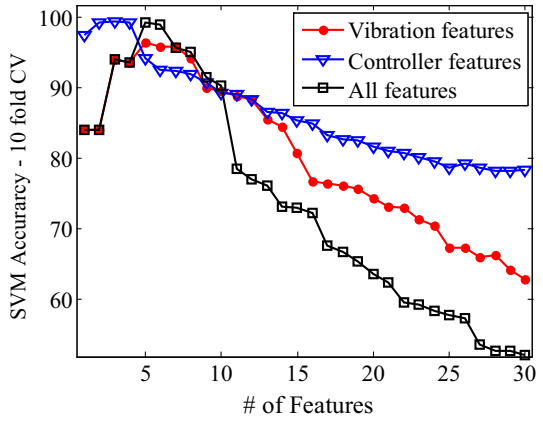

Fig. 7. Fine selection of the optimal feature set for early diagnosis.

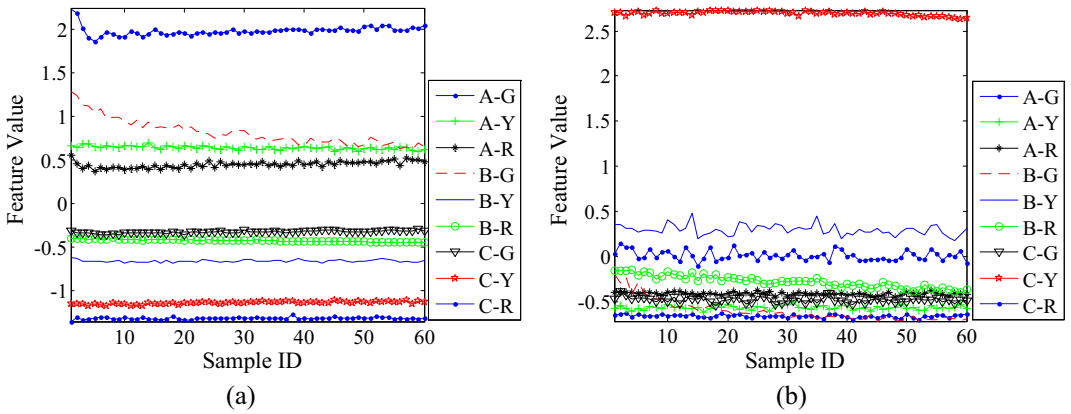

Fig. 8. The best ranking feature from (a) torque signal (b) vibration signal at ball nut.

multi-class classification problems. Also, that is the reason why the subsequent wrapper selection method is introduced to mitigate this bias.

To further investigate the accuracy of early diagnosis, the confusion matrices of three SVM classifiers, based on different optimal feature sets, are presented in Fig. 9. In experiment 1, each of the 9 tests is conducted for one hour and 60 date files are collected during the test. Therefore, there are a total 540 data files for the experiment 1. In the classification test, 50 data

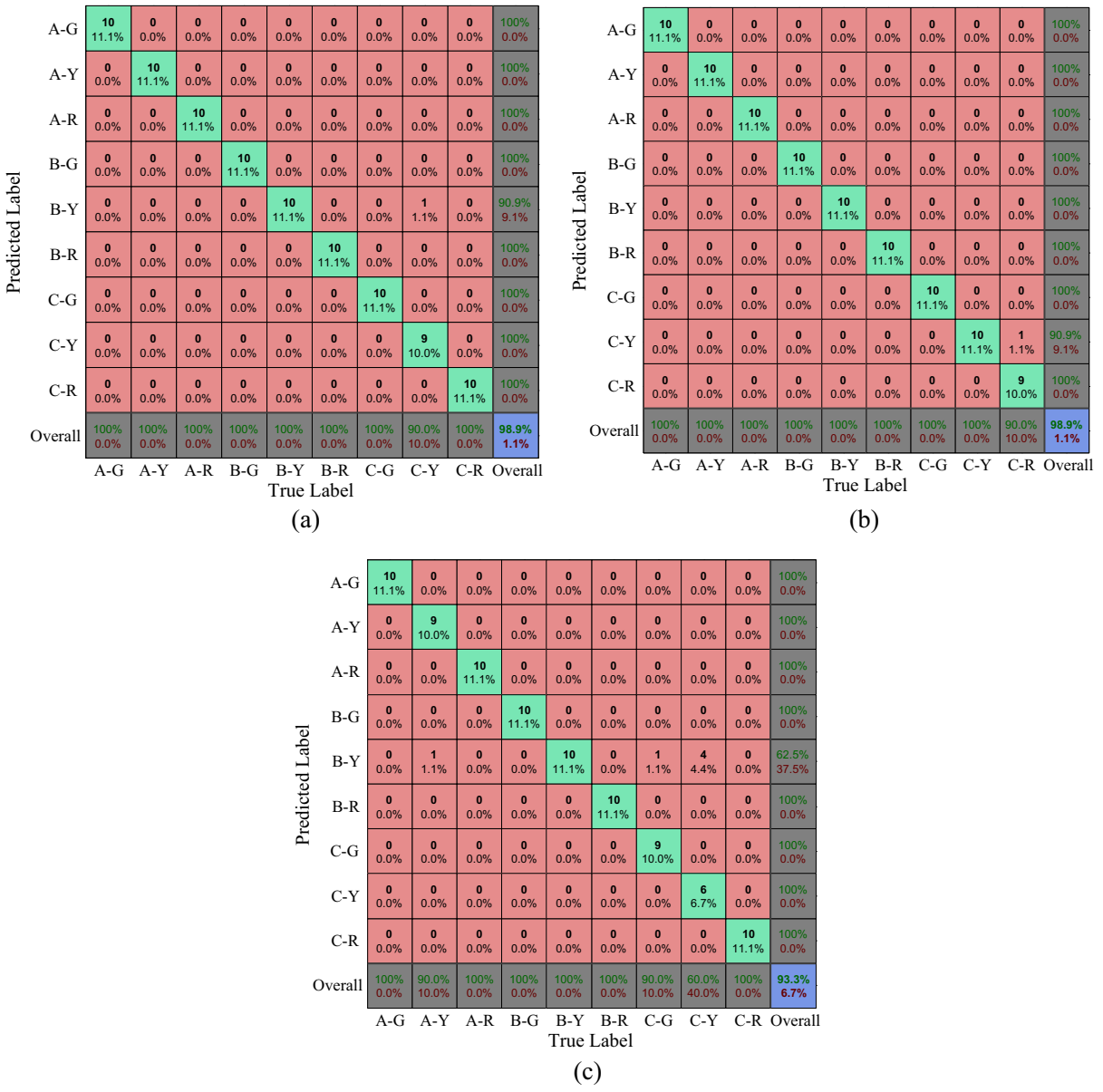

Fig. 9. Confusion matrix for the early diagnosis of ball screw assembly based on the optimal feature set selected from (a) all features; (b) controller features; (c) vibration features.

files are randomly selected from each of the 9 classes to build a training data set, and the remaining data files are used for testing. Then the predicted class labels for the testing data set would be compared with the true class labels to calculate the final accuracy and construct the confusion matrix. In Fig. 9(a), the input features for the classifier are defined as the optimal input feature set selected from all the features. These features include 4 vibration features and 2 torque features. And the final accuracy is 98.9%. Similarly, the optimal controller feature set, made up of the top 4 features from all controller features, achieves the same overall accuracy as 98.9% and only 1 data sample is misclassified. In comparison, the optimal vibration feature set, consisting of the top 6 vibration features, shows a higher rate of misclassification with 5 data samples. These results further indicate that the controller data may be superior to the vibration data in terms of early diagnosis. Therefore, the sensor-less strategy for PHM implementation is recommended in future investigations.

The first 2 principal components for the three optimal feature sets are extracted and plotted individually in Fig. 10. From the scatterplot, one can easily find that the optimal feature set for all the features and for the controller features in Fig. 10(a) and (b) can both separate all 9 classes without any mixed samples. However, Fig. 10(c) represents many mixed samples in some of the classes and that's why the classification accuracy for the vibration features are not as good as the other two scenarios.

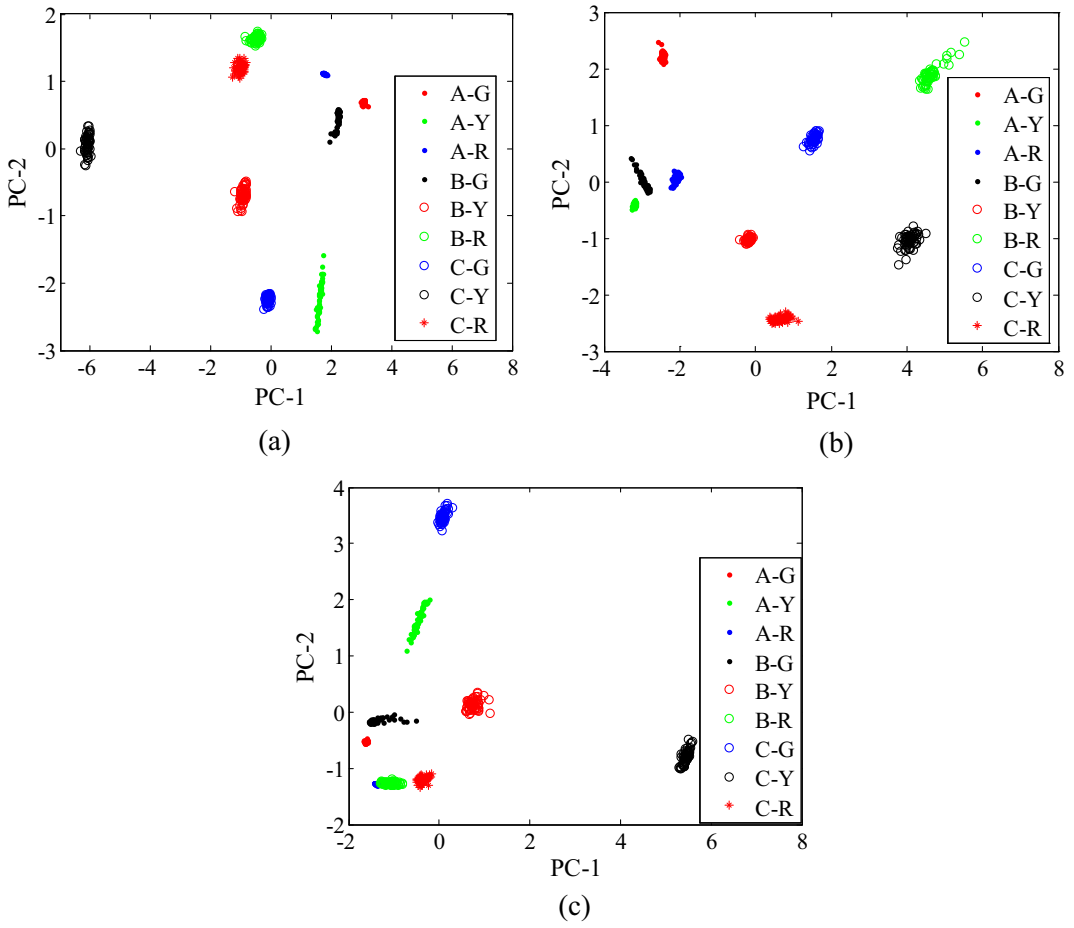

Fig. 10. Principal components of optimal feature set selected from the (a) all the features; (b) controller features; (c) vibration features.

4.2. Case study 2: accelerated life test

According to the proposed feature selection strategy for prognosis in Fig. 5, a few undesired features would be filtered using criterion in early diagnosis situation. Then the feature ranking based on the slope value in the ALT experiment is presented in Fig. 11. In Fig. 11, one can easily see that the top-ranking vibration features and all features are exactly the same, which indicates that most of the controller features do not have very good monotonic trend. To explain this observation, the top-ranking features that are extracted from vibration signal and torque signal are shown in Fig. 12. Fig. 12(a) shows the 1st ranking feature that represents the ball nut vibration, which shows a very nice upward trend to indicate the ball screw degradation. The vibration level starts to rise slowly since the beginning of the ALT, and increases drastically after 556 h of running. On the other hand, the representative torque feature decreases slowly since the ALT begins, but rises suddenly at 556 h, as shown in Fig. 12(b). The slow degradation in torque signal at the beginning of ALT matches well with the analysis in the previous experiment. However, the sudden rise in the torque signal at 556 h is possibly caused by the jamming of the metal debris. During the experiment, a significant amount of metal debris was found in the lubrication oil and also a very sharp noise is heard from the test bed around this time. Therefore, it is believed that the metal debris jammed the moving trajectory of the rolling elements and interrupted the slow downward trend of the torque signal.

Another point of discussion concerns the ball nut vibration feature in Fig. 12(a) and in Fig. 8(b). It is found that in Fig. 12(a) the ball nut vibration level rises very slowly at the beginning but drastically towards the end. This explains why the vibration feature in Fig. 8(b) is not as good as the torque signal in terms of early fault diagnosis. However, it's noted that the classification accuracy of 93.3% based on the vibration signal is pretty high, which is also acceptable for industrial applications. Also, the torque signal is found to be quite useful for early fault diagnosis when the ball screw is running without a load and sufficient lubrication is provided throughout the experiment. As for the harsh operation condition in experiment 2, the possible disturbance of the generated debris inside the ball nut would weaken the torque's ability for tracking the whole degradation process of the ball screw. Therefore, vibration monitoring has more value for degradation assessment as well as early fault identification. When vibration signal is not available, the torque signal also holds value

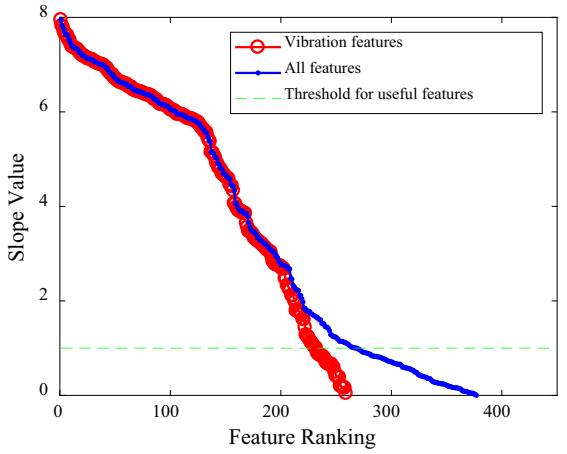

Fig. 11. Feature ranking based on slope value.

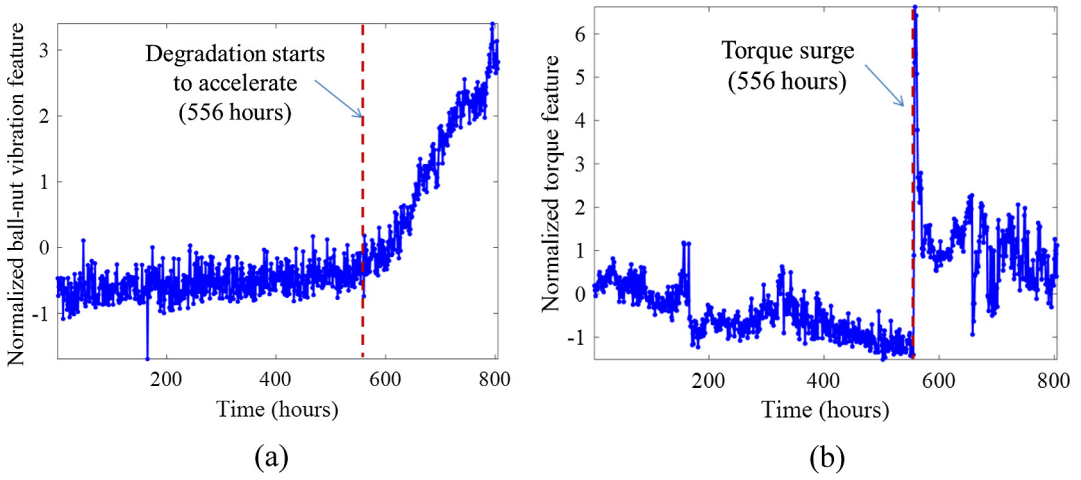

Fig. 12. Top ranking features extracted from vibration signal (a) and torque signal (b).

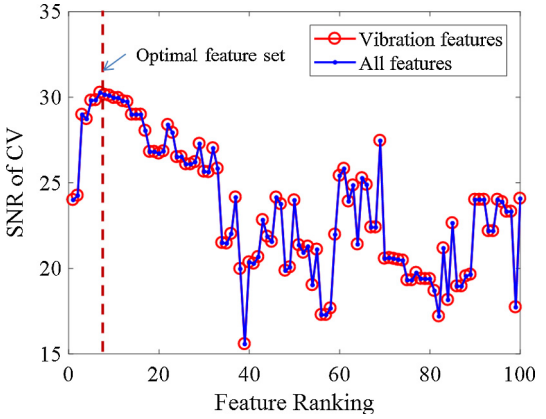

Fig. 13. Selection of the optimal feature set for health assessment.

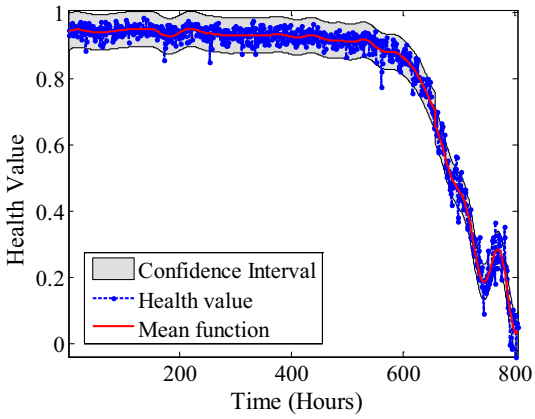

Fig. 14. Health assessment results based on GPR.

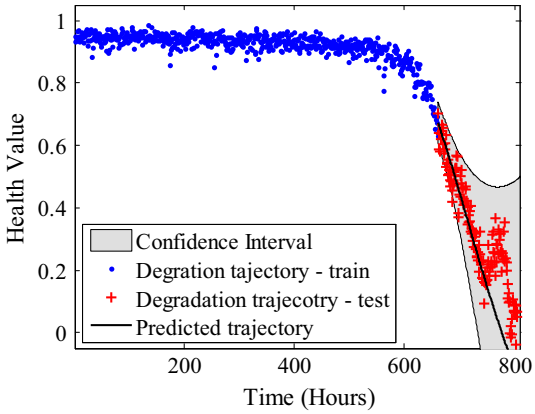

Fig. 15. Remaining useful life prediction using GPR.

in capturing the early fault signature. The result in ALT in Fig. 12(b) indicates that the torque signal is also useful in detecting the jammed failure or the presence of metal debris.

To select the optimal feature set for health assessment, the SNR of the health value series given by linear regression is used to evaluate the performance of the input feature set, as shown in Fig. 13. It is found that the selected features in the optimal feature set for health assessment are all vibration features. And the degradation trajectory based on the optimal feature set is shown in Fig. 14, which clearly has an exponential degradation trend. When computing the SNR of the health value series, the mean function is extracted by using GPR, as shown in Fig. 14.

To predict the RUL based on the ball screw degradation trajectory, the GPR is employed to make the prediction. In the setting of analysis, 80% of the whole trajectory is employed for training and the remaining 20% for testing, the kernel matrix for GPR is set as squared exponential. The prediction result and the confidence interval are presented in Fig. 15 which indicates that there is a very good agreement with the future propagation of degradation. The predicted life span for the ball screw is 780 h, which is close to the actual life span of 800 h. The result demonstrates the predicted RUL is accurate.

5. Conclusions

In this paper, a systematic methodology for a ball screw prognosis analysis is proposed and experimental investigations are designed to study the availability of ball screw prognosis as well as to demonstrate the effectiveness of the proposed methodology. It is found that the proposed method can be a promising tool for ball screw early fault diagnosis, degradation assessment and RUL prediction. In addition, this study also compares the performance of a sensor-less strategy and a sensor-rich strategy in terms of the ball screw PHM. The analysis results demonstrate that the built-in torque signal is valuable for fault diagnosis and incipient failure identification. However, the presence of metal debris may introduce complexity to the signal analysis and also impair the practicality of using torque signal only for PHM implementation. This needs to be carefully considered in real-world applications. On the other hand, the vibration signal demonstrates a clear exponential

degradation trend of the system, but it is a bit less sensitive than the torque signal to diagnose incipient fault. The vibration based PHM analysis is found more robust than the torque based PHM analysis regarding the presence of metal debris.

For the future works, strategies to make the torque signal-based PHM more robust and practical will be further explored. The primary focus would be on the extraction of the robust features from torque signal using advanced techniques. Also, health monitoring based on advanced sensing devices, such as Integrated Measurement Unit (IMU) [25,26], will be benchmarked with data-driven method.

References

[1] J.L. Chang, J. Chao, Y. Huang, J. Chen, Prognostic experiment for ball screw preload loss of machine tool through the Hilbert-Huang Transform and Multiscale entropy method, Information and Automation (ICIA), pp. 376–380, IEEE International Conference on 2010.
[2] G.-H. Feng, Y.-L. Pan, Establishing a cost-effective sensing system and signal processing method to diagnose preload levels of ball screws, Mech. Syst. Sig. Process. 28 (2012) 78–88.
[3] P. Tsai, C. Cheng, Y. Hwang, Ball screw preload loss detection using ball pass frequency, Mech. Syst. Sig. Process. 48 (2014) 77–91.
[4] W. Jin, Y. Chen, J. Lee, Methodology for ball screw component health assessment and failure analysis, ASME 2013 International Manufacturing Science and Engineering Conference collocated with the 41st North American Manufacturing Research Conference, 2013, pp. V002T002A031–V002T002A031.
[5] J. Cuttino, T. Dow, B. Knight, Analytical and experimental identification of nonlinearities in a single-nut, preloaded ball screw, J. Mech. Des. 119 (1997) 15–19.
[6] J. Lee, F. Wu, W. Zhao, M. Ghaffari, L. Liao, D. Siegel, Prognostics and health management design for rotary machinery systems—reviews, methodology and applications, Mech. Syst. Sig. Process. 42 (2014) 314–334.
[7] X. Jia, C. Jin, M. Buzza, Y. Di, D. Siegel, J. Lee, A deviation based assessment methodology for multiple machine health patterns classification and fault detection, Mech. Syst. Sig. Process. 99 (2018) 244–261.
[8] G.-H. Feng, Y.-L. Pan, Investigation of ball screw preload variation based on dynamic modeling of a preload adjustable feed-drive system and spectrum analysis of ball-nuts sensed vibration signals, Int. J. Mach. Tools Manuf. 52 (2012) 85–96.
[9] X. Jia, M. Zhao, Y. Di, C. Jin, J. Lee, Investigation on the kurtosis filter and the derivation of convolutional sparse filter for impulsive signature enhancement, J. Sound Vib. 386 (2017) 433–448.
[10] Y.-C. Huang, S.-L. Sun, K.-H. Peng, Ball nut preload diagnosis of the hollow ball screw through sensed current signals, Int. J. Automat. Smart Technol. 4 (2014) 134–142.
[11] X. Jia, C. Jin, M. Buzza, W. Wang, J. Lee, Wind turbine performance degradation assessment based on a novel similarity metric for machine performance curves, Renew. Energy 99 (2016) 1191–1201.
[12] F. Li, Y. Jiang, T. Li, Y. Du, An improved dynamic model of preloaded ball screw drives considering torque transmission and its application to frequency analysis, Adv. Mech. Eng. 9 (2017), 1687814017710580.
[13] J.-S. Chen, Y.-K. Huang, C.-C. Cheng, Mechanical model and contouring analysis of high-speed ball-screw drive systems with compliance effect, Int. J. Adv. Manuf. Technol. 24 (2004) 241–250.
[14] W.G. Lee, J.W. Lee, M.S. Hong, S.-H. Nam, Y. Jeon, M.G. Lee, Failure diagnosis system for a ball-screw by using vibration signals, Shock Vib. 2015 (2015).
[15] Hiwin Ballscrews Technical Information, Hiwin Technology Company, Taiwan, 2016.
[16] Hiwin Linear Guideway Technical Information, Hiwin Technology Company, Taiwan, 2016.
[17] R. Yan, R.X. Gao, X. Chen, Wavelets for fault diagnosis of rotary machines: a review with applications, Signal Process. 96 (2014) 1–15.
[18] M. Zhao, X. Jia, J. Lin, Y. Lei, J. Lee, Instantaneous speed jitter detection via encoder signal and its application for the diagnosis of planetary gearbox, Mech. Syst. Sig. Process. 98 (2018) 16–31.
[19] M. Zhao, X. Jia, A novel strategy for signal denoising using reweighted SVD and its applications to weak fault feature enhancement of rotating machinery, Mech. Syst. Sig. Process. 94 (2017) 129–147.
[20] X. Jia, M. Zhao, M. Buzza, Y. Di, J. Lee, A geometrical investigation on the generalized l p/l q norm for blind deconvolution, Signal Process. 134 (2017) 63–69.
[21] I. Guyon, A. Elisseeff, An introduction to variable and feature selection, J. Mach. Learn. Res. 3 (2003) 1157–1182.
[22] E. Schubert, A. Zimek, H.-P. Kriegel, Generalized outlier detection with flexible kernel density estimates, in: Proceedings of the 2014 SIAM International Conference on Data Mining, SIAM, 2014, pp. 542–550.
[23] L. Liao, W. Jin, R. Pavel, Enhanced restricted Boltzmann machine with prognosability regularization for prognostics and health assessment, IEEE Trans. Ind. Electron. 63 (2016) 7076–7083.
[24] I.H. Witten, E. Frank, Data Mining: Practical Machine Learning Tools and Techniques, Morgan Kaufmann, 2005.
[25] G.W. Vogl, B.A. Weiss, and M.A. Donmez. A sensor-based method for diagnostics of machine tool linear axes, in: Proceedings of the Annual Conference of the Prognostics and Health Management Society, Prognostics and Health Management Society, Conference, vol. 6. NIH Public Access, 2015.
[26] G.W. Vogl, M.E. Sharp, Diagnostics of Machine Tool Linear Axes Via Separation of Geometric Error Sources, 2017.